

Using fractal dimension to evaluate alveolar bone defects treated with various bone substitute materials

Research Article

Marcin Kozakiewicz¹, Sławomir Chaberek²,
Katarzyna Bogusiak^{3*}

*1 Department of Maxillofacial Surgery, Medical University of Lodz,
ul. Zeromskiego 113, 90-549 Lodz, Poland*

2 Independent Clinical Hospital, ul. Konarskiego 13, 05-400 Otwock, Poland

*3 Department of Craniomaxillofacial and Oncological Surgery, Medical University of Lodz,
ul. Kopcińskiego 22, 90-153 Lodz, Poland*

Received 6 January 2013; Accepted 22 April 2013

Abstract: Introduction: This study analyzed how different implanted materials affected the healing of alveolar defects using fractal dimension (FD) computation taken from radiographs. Methods: 236 patients with bone defects in the upper/lower jaw were selected to this study and treated with: algae derived hydroxyapatite (AHA), bovine bone mineral (BBM), beta-tricalcium phosphate (TCP), synthetic hydroxyapatite (SHA), biological active glass (BAG), autogenous bone grafts (ABG), reference group (REF) – intact bone. 22 patients with bone defects where the bone substitute was not introduced made NON group. The results were monitored using intraoral x-ray imaging. Results: FD varied with the different biomaterials throughout the time of observation and reflected individual character of bone remodeling. Fractal analysis of intact and augmented bone during observation showed higher FD for the intact bone in comparison with the biomaterials site. Conclusions: Fractal techniques can be a descriptor of bone substitutes. On the basis of the differences in the dynamics of alteration between different bone substitute materials we can distinguish two groups of them. Visible changes in the structure emerge earlier in places of implantation of BBM and TCP in comparison to the group of biomaterials constituting more stable patterns of radiotexture: AHA, BAG, SHA.

Keywords: *Biocompatible Materials • Bone Resorption • Bone Substitutes • Fractal analysis • Image Processing • Mandible • Maxillary Sinus • Subtraction Technique*

© Versita Sp. z o.o.

1. Introduction

Augmentation of bone defects by insertion of graft materials is an excellent method to construct a suitable bony bed for implant placement [1,2]. Based on origin, bone replacement materials (BRM) are classified as allogenic, heterologous and alloplastic ones [3]. Clinical and pathological evidences from many studies indicate that the use of an autogenous bone is favored as a gold standard [4,5]. However, there are many problems associated with harvesting an adequate quantity of the autogenous bone, two sites morbidity in the patient, and brought together complications. These factors cre-

ate barriers for the widespread use of autogenous bone transplantation. The availability of suitable biomaterials to be used as a bone replacement that facilitates the bone regeneration would eliminate the need for a second surgical site.

A crucial differentiating feature of the synthetic material depends not only on the origin, but also the surface characteristic and the degree of the porosity [6,7]. Also, the process of bone ingrowth depends on the size of pores in the BRM scaffold. The heterologous materials are obtained through the processing of bone derived from different species, such as material derived from bovine bone (BBM). Alloplastic materials are constituted by

* E-mail: katarzyna.bogusiak@gmail.com

synthetic composites, such as: biologically active glass (BAG), e.g. Biogran, PerioGlass; tricalcium phosphate particles (TCP), e.g. Cerasorb, Bioresorb, Chronos, Bio-base; and hydroxylapatite (SHA), e.g. Ha-Biocer.

BBM is comprised of multi-shaped grains, 1-2 mm in size. Because of its considerable size, changeable gradability and macroporosity in bone defect, the material may constitute spatial macroporosity system in implantation site. The surface of the material is practically devoid of micropores, which considerably restricts resorption, together with its chemical composition of hydroxylapatite. Research shows phenomenon that even after two years after implantation, the material displays higher density than on the day of surgery and higher than in surrounding bone. This is an osseointegrating material which exhibits long term stability in the organism after interbone implantation. It has osteoconductive capacity. It is used primarily in periodontology and oral implantology [8].

By contrast, beta-tricalcium phosphate $\beta\text{-Ca}_3(\text{PO}_4)_2$ is subject to very fast and full resorption. About 80% undergoes resorption 7 months after implantation. This may be considered a flaw, since bone tissue development may be slower than biological degradation, which results in the ingrowth of new bone. TCP is built of round grains 1-2 mm in size, which show roughness and porosity of the surface. The material manifests short stability in organisms after endosteal implementation [9].

SHA, i.e. synthetic hydroxylapatite, has very limited resorption rate. Collagen fibers generated by osteoblasts first form the zone of contact between the surface of hydroxylapatite, which contains calcium, and then cells forming the bone [10].

BAG, i.e. biologically active glass, originates from silicon oxides, sodium oxides, calcium oxides and phosphorous oxides (and differ in the size of particles 90-360 μm) [11]. As a result of their contact with tissue fluids, the glass gives off ions, thanks to that cracks develop and increase porosity. Biologically active glass is widely popular in dentistry and yields positive results in periodontology [12].

ABG, i.e. autogenous bone grafts, are harvested from the oral cavity approach, most frequently from the mandible (a cortical bone characterized by a long resorption time) or from hip bone (a cancellous bone characterized by a shorter resorption time). All bone transplants are subject to restructuring, with resorption dominating. It is not clear whether, depending on the degree of restructuring, new differences arise concerning mechanical features of bones in sites of regeneration, particularly in the case of a cancellous bone [13].

There are also biological purely plant-based biomaterials, such as calcium carbonate derived from marine

algae (Algipore). It is obtained from natural carbonate calcium incrustated algae, and after chemical transformation (98%) it is comprised of hydroxylapatite. This material shows great porosity (porous diameter approximately 200 μm). However, after it is used, the growth of bone tissue is not always observed. The possibility of full bone transformation is a moot point among researchers. Additionally, algae derived hydroxylapatite (AHA) displays a very long resorption time, as it is decomposed by osteoblasts very slowly. The estimated resorption time is 7 years [14].

All these bone substitute materials possess different resorption rates, chemical and structural characteristics and their influence on stimulation or support of bone regeneration differs. For the clinician it would be valuable to assess the bone regeneration after the implantation of different biomaterials. The effect of various grafts including allogenic bone, alloplastic bone substitutes and their combinations [15-19,20,21] have been extensively studied in animal models [22-25,26] and in vitro experiments [27,28]. There has also been research assessing the augmentation process with the use of clinical, histological and histomorphometrical analysis in humans [29]. Roentgenographic examination of the bone defect healing process in humans after introducing a bone substitute material using only one's sight has a subjective character. Extensive research has been conducted according to objective radiological methods assessing trabecular structure on the basis of mathematical analysis of bone texture, like microdensitometry, subtraction radiography [30,31]. Another mathematical description method of the structural pattern of trabecular bone is fractal analysis. This quantitative method measures complex geometric structures that exhibits self-symmetry throughout the image [32,33]. The complexity of the structure is represented by the fractal dimension; with its increasing number the complexity increases [34]. There are many methods of fractal analysis. They are mathematically different and give rise to various numerical values. The results of such evaluation would only be the same in the case of identical fractal surfaces (continuous and self-similar). Fractal dimension (FD) is a numerical expression for describing complex shapes and structural patterns [35]. There are two methods of fractal dimension calculation: spatial and spectral. The first type operates in the spatial domain (Box Counting Method, Intensity Variance Method, Variation Method, and Blanket Method). The second type operates in the frequency domain, using the Fourier power spectrum. This method was also used by Ruttimann et al. [35], Law et al. [36] on dental radiographs of postmenopausal women, and Samarabandu et al. [37] on rat femurs. In dentistry, fractal dimension on periapical radiographs has been used as a simple descriptor

of the complex architecture of the cancellous bone surrounding the dentition [35,38]. The technique appears to be relatively insensitive to variations in film exposure or alignment [1,37,39,40] and is relatively independent of technical settings of periapical radiographs [41] but is affected by the size and shape of the regions of interest [1]. Fractal dimension has been shown to distinguish patients with gingivitis and periodontitis [42] and those with and without osteoporosis [25] and has been used for assessment of dental implant sites [43]. A method of computing fractals based on Fourier's two-dimensional power spectrum was used in cases when crucial information about the degree of structural systematicity depended on the direction and size of the structures analysed [34,44-46].

These studies show the potential capabilities of fractal analysis in analyzing trabecular bone structure on the basis of retrospective periapical radiographs. However, there is no report comparing bone substitutes in long-term assessment with the use of fractal analysis.

The aim of this study was to analyze how different implanted materials affected the healing of alveolar defects using fractal dimension (FD) computation taken from radiographs acquired 1, 2 and 3 years after the oral surgery.

2. Materials and methods

Two hundred and thirty six patients were included into this study (female: 131, male: 105; mean age 35.9±13.7 years). All patients were in good physical health and had no addictions. They demonstrated an acceptable level of oral hygiene. Those patients had postoperative 5-wall defects created in the course of operative treatment of jaw cyst enucleations, tooth removals, apicoectomies or bone harvesting. This study was approved of by the Institutional Review Board (IRB) – RNN/91/02/KE.

The defects of the jaw bone were treated with: algae derived hydroxyapatite (AHA - 48 cases), bovine bone mineral (BBM – 24 cases), beta-tricalcium phosphate (TCP – 34 cases), synthetic hydroxylapatite (SHA – 22 cases), biologically active glass (BAG – 34 cases), autogenous bone grafts (ABG – 20 cases), reference group – intact bone, sites in edentulous ridges (REF: 32 cases). There has also been a control group of 22 patients with bone defects, (tooth root extraction without a pre-planned implant surgery or place from which a patient's bone sample has been taken) where the bone substitute was not introduced (NON - 22 cases). Digital intra-oral radiographs were taken 4 times: at 12 months' (M) intervals (00M, 12M, 24M, and 36M) during follow-up examinations. Therefore, the analysis was based on

exactly 944 images (236 patients with 4 radiographs each). The images were acquired (during standard clinical procedures) by the same person, with similarly positioned reference points by one operator. The images were taken with the use of the right angle technique. The Digora Optime system of digital radiography (Soredex, Tuusula, Finland) was applied in this study [47]. Radiographs were taken in a standardized way. It was applied a modified RINN system, from which we utilized the ring for tube fixation and film plate holder (vertical and horizontal). The ring was placed in roentgen apparatus and fixed to the film plate holder connected by the horizontal bar. The ring in the roentgen apparatus was joined by additional adapting ring that was rigidly fixed to the X-ray tube. We applied enveloped storage phosphor plate with a step wedge with thickness 0.1, 0.2, 0.4, 0.8 mm of copper. A bite index was prepared with a silicone material (occlusal bite duplicates the shape of film plate holder and also occlusal surfaces of the teeth). The X-ray detector was placed in the RINN positioner and the bite index with the connection bar was replaced in the mouth of the patient and fixed to the tube. The same radiological apparatus was used: Focus X-ray intraoral unit (Instrumentarium Dental, Tuusula, Finland). Technical parameters of exposure were the same in all included radiographs: 7 mA, 70 kV and 0,06 s. Adobe Photoshop 7.0 software was used to select and choose ROI images (region of interest) consisted of 64x64 pixels of 256 grey levels (Figure 1). The pixel size equated to 70 µm. ROIs analyzed were located in the same anatomical area throughout the time of observation. The best possible approximation of anatomical location was assured thanks to standardized method of radiographs acquisition and also thanks to the fact that ROIs were placed within identical reference points for each patient. As a reference point, we chose anatomical structures placed within an intact area without lesions. ROIs were placed on the most central part of bone defects without any anatomical structures imposed. The ROI were separated and saved as a bitmap file on the PC. We used the spectral method, frequency domain technique method to calculate the fractal dimension. The decision to choose this method was preceded by a careful investigation of biological processes taking place in the structure under study, as well as its construction and functioning. The choice of the methods of analysis and assessment of results were also affected by assumptions and goals we defined.

An automatic algorithm was written using Mathcad Plus 6.0 software (PTC, USA, Needham) for mathematical analysis. This program was based on the Fourier power spectrum method (Figure 1 a,b,c,d) and allowed Fast Fourier Transform (FFT) coefficients and fractal

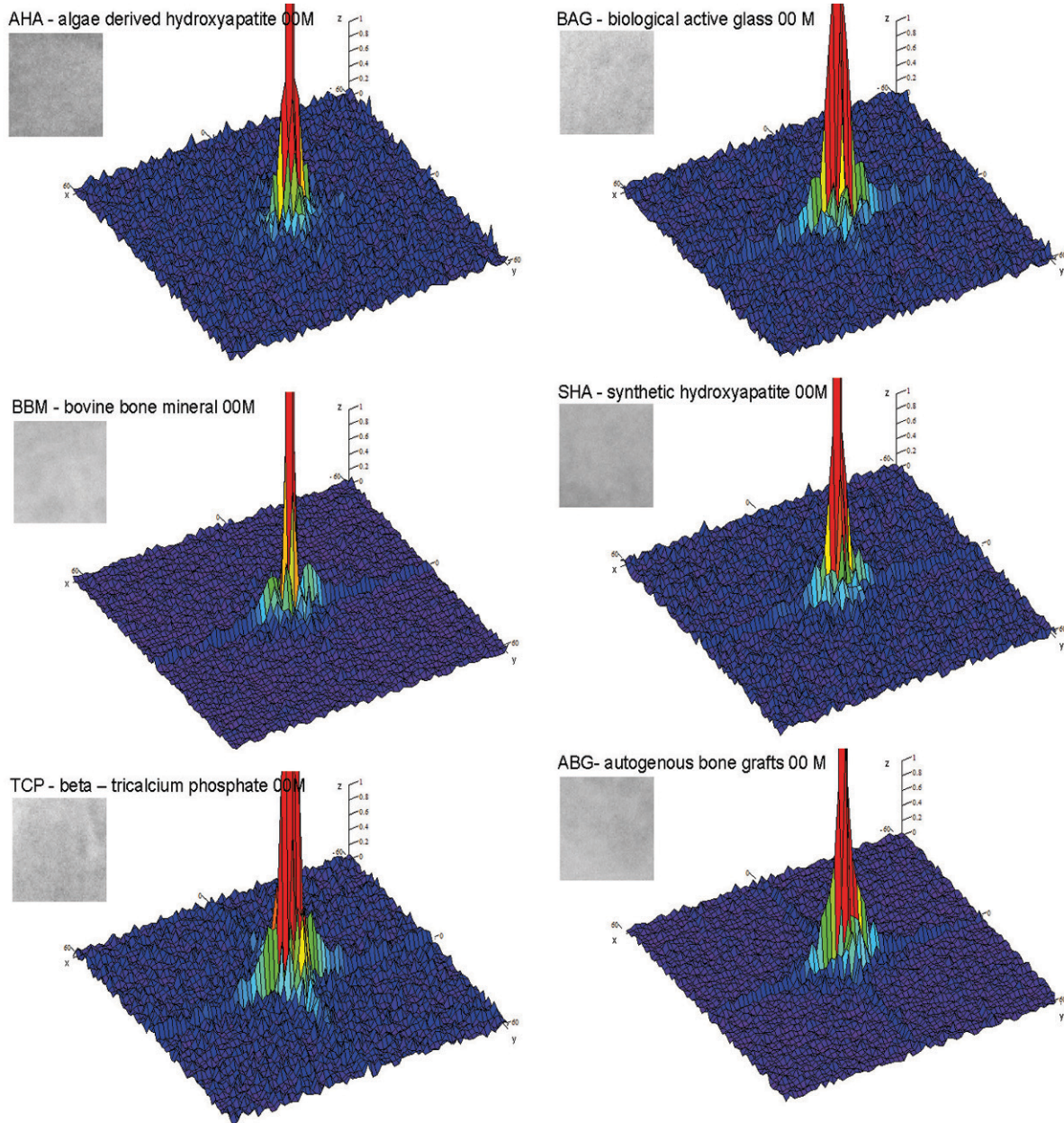


Figure 1a. Results of Fourier Transformation: 3 dimension presentation of amplitude distributions the Fourier Transformation of analysed images; (axes: x,y – spatial frequencies, z – amplitude). Abbreviation: 00M – state immediately after operation.

dimension calculations. Firstly, in this method the calculation of the two-dimensional Fourier transform of the digital image is done, and two-dimensional power spectrum is obtained. The two dimensional power spectrum can be averaged by means of sampling the spectrum in the area of rings of defined width Δf , for all frequencies f [38,44]. Calculations were performed for rings of a given width Δf each ($\otimes f = 1,01$ 1/mm). Thus the energy spectrum contained information concerning

the structures of interest included in the scope of spatial frequencies, from f to $n \cdot \otimes f$, grouped in packets of width equal to $\otimes f$. The boundary frequencies of given rings can be determined, based on the following dependency, where P_n is the mean value of the spectrum of the two dimensional Fourier transform for n ring of a given width Δf each:

$$(n-1) \cdot \Delta f \leq f P_n \leq n \cdot \Delta f.$$

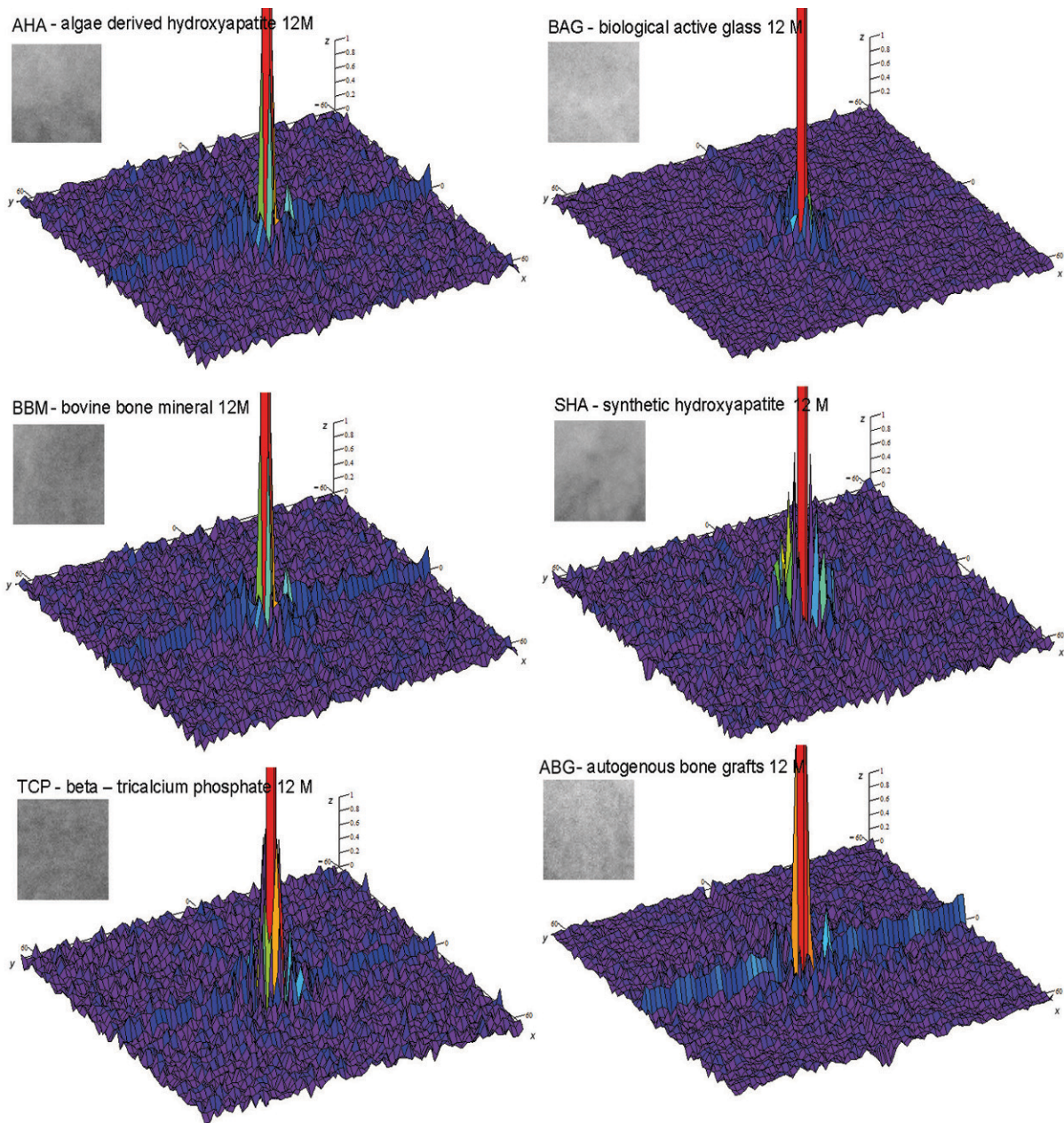


Figure 1b. Results of Fourier Transformation: 3 dimension presentation of amplitude distributions the Fourier Transformation of analysed images; (axes: x,y – spatial frequencies, z – amplitude). Abbreviation: 12M – twelve months after surgery.

Then, the two-dimensional power spectrum is reduced to one dimension by averaging over lines. The average one-dimensional power spectrum $P(f)$ of the surface is a function of the frequency f :

$$P(f) = k f^\beta.$$

When the $\log(P(f))$ is plotted against $\log(f)$, a slope of the least-squares linear regression of the logarithmic

plot of $P(f)$ versus f is equal β .

$$\begin{aligned} \beta &= (-1 - 2H) \\ P(f) &= k f^{(-1-2H)} \\ H &= -(1+\beta)/2. \end{aligned}$$

The fractal dimension of the region is:

$$\begin{aligned} FD &= 3 - H \\ FD &= (7 + \beta)/2. \end{aligned}$$

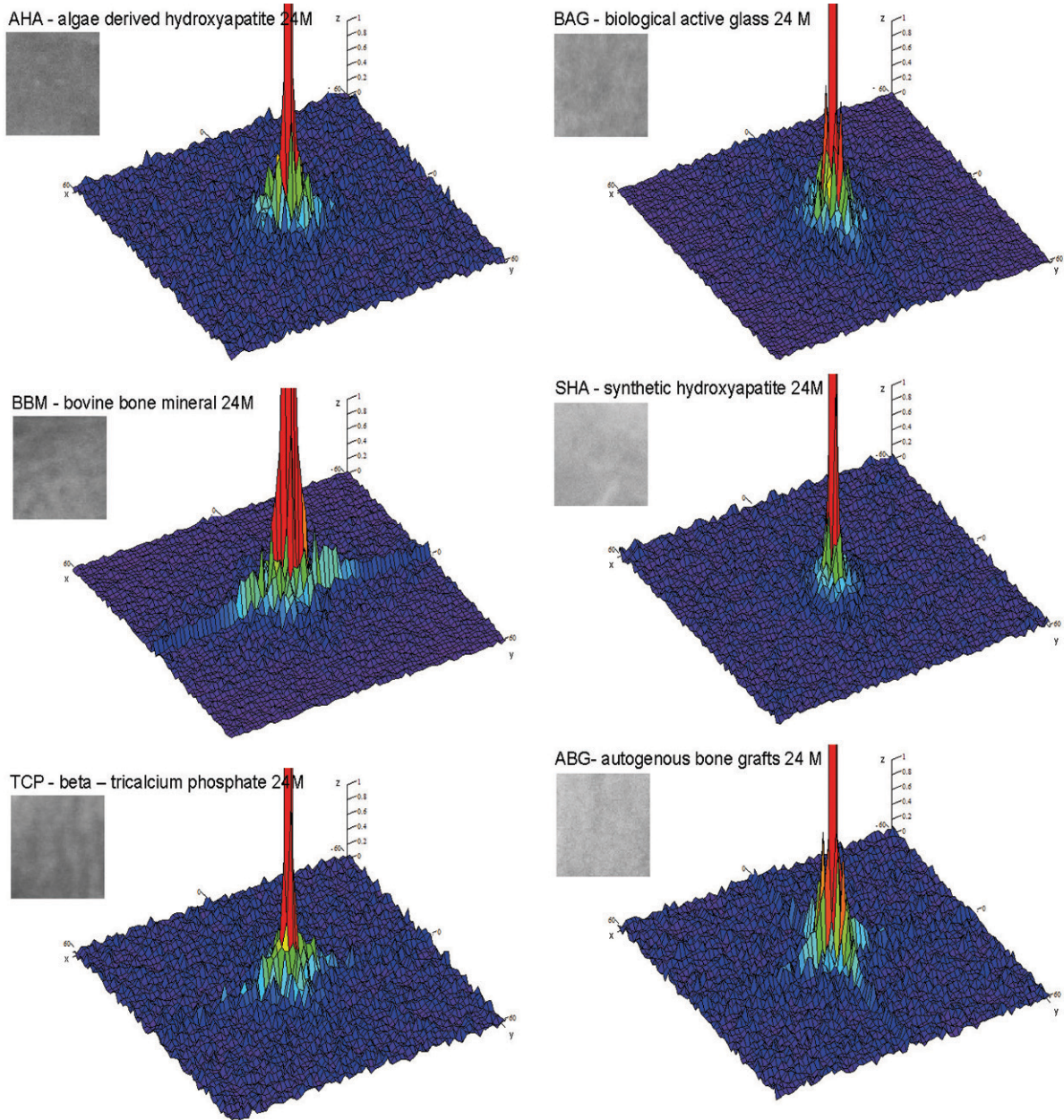


Figure 1c. Results of Fourier Transformation: 3 dimension presentation of amplitude distributions the Fourier Transformation of analysed images; (axes: x,y – spatial frequencies, z – amplitude). Abbreviation: 24M – twenty four months after surgery.

In the case of homogenous structure, the amplitude spectrum of Fourier transform is largest in the regions of low spatial frequencies, the H coefficient (Hurst coefficient) attains high values, and thus the corresponding fractal dimension is low. For the heterogeneous structures, i.e. the ones characterized by a more evenly distributed amplitude spectrum, the H values are low and the corresponding fractal dimension attains a large value [48,49].

2.1 Statistical analysis

For the reason that data distribution differed significantly from normal distribution, non-parametric tests were applied. The Kruskal – Wallis one – way analysis of variance was used to determine the statistical significance of differences among analyzed groups of patients. The Mann–Whitney test was then used as a post-hoc test. A two factor analysis of variance (time and group of patient) was done with the ANOVA Friedman test.

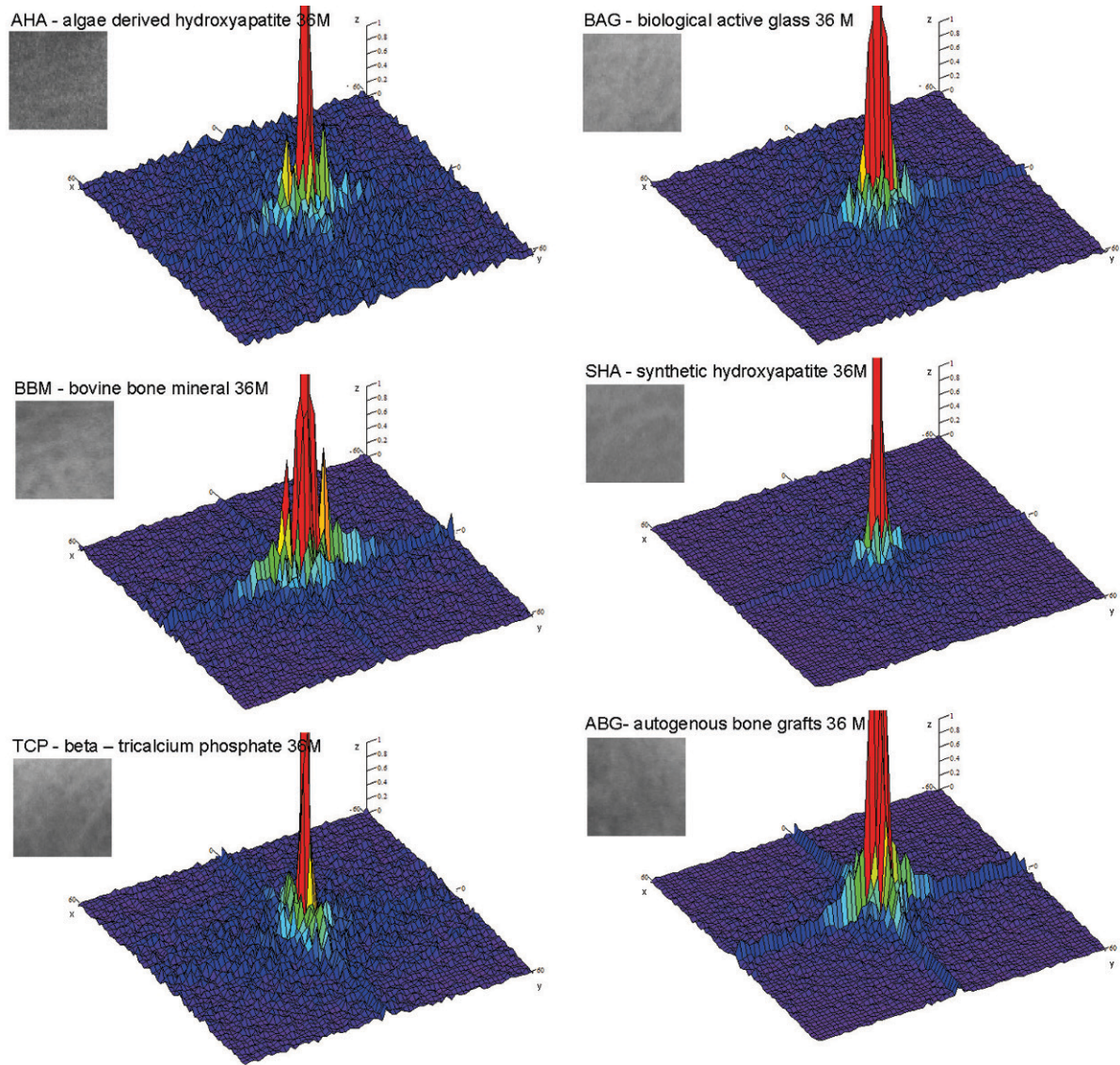


Figure 1d. Results of Fourier Transformation: 3 dimension presentation of amplitude distributions the Fourier Transformation of analysed images; (axes: x,y – spatial frequencies, z – amplitude). Abbreviation: 36M – thirty six months after surgery.

As a post-hoc test we used Wilcoxon signed-rank test. The critical p value for null hypothesis rejection was set at $p=0.05$ (Statgraphics Centurion XVI, Statpoint Technologies, Inc., Virginia, USA).

3. Results

In case of spontaneously healed defect [NON] the averages of FD immediately after surgery were significantly higher than in each of the following periods of the study ($p < 0.01$; $p < 0.05$). Values of fractal dimension of algae derived hydroxylapatite after 12 and 36 months of observation took on average significantly

lower values than in the baseline examination ($p < 0.001$). Also, the results after 36 months were significantly lower than after 24 months ($p < 0.01$) for this biomaterial (Table 1). Fractal dimension values calculated for SHA in the observed periods were fairly similar and the possible significance of the error rate was $p=0.055$. Detailed analysis in different periods of observation disclosed that after 36 months FD values were significantly lower than after 12 and 24 months ($p < 0.05$). The comparison of the results in the BAG group gave similar results as in the AHA group. It turned out that the difference in results over time was statistically significant, although at a greater level of error ($p < 0.05$), but similarly in the

Table 1. Fractal dimension of the image of bone defect filled with different bone substitutes. 36 months follow-up.

Materials	Examination time	Calculated parameters of fractal dimension (FD)						
		min	max	x	Me	Q _x	SD	v (%)
AHA	0M	2,265	2,598	2,421	2,421	0,032	0,0577	2,38
	12M	2,415	2,296	2,417	2,415	0,030	0,0423	1,75
	24M	2,227	2,503	2,402	2,402	0,033	0,0565	2,35
	36M	2,238	2,517	2,364	2,340	0,052	0,0732	3,10
	Comparison (significant differences)							
				chi ² =20,075; p<0,001				
				0 with 36: z=4,492; p<0,001				
				12 with 36: z=3,964; p<0,001				
				24 with 36: z=3,154; p<0,01				
NON	0M	2,285	2,493	2,424	2,419	0,031	0,0503	2,07
	12M	2,309	2,492	2,389	2,384	0,025	0,0422	1,76
	24M	2,301	2,440	2,390	2,397	0,025	0,0376	1,57
	36M	2,214	2,476	2,367	2,369	0,063	0,0737	3,11
	Comparison (significant differences)							
				chi ² =15,055; p<0,01				
				0 with 12: z=2,646; p<0,01				
				0 with 24: z=2,760; p<0,01				
				0 with 36: z=2,549; p<0,05				
SHA	0M	2,223	2,521	2,382	2,389	0,048	0,0671	2,82
	12M	2,272	2,472	2,404	2,414	0,028	0,0433	1,80
	24M	2,280	2,477	2,400	2,404	0,029	0,0478	1,99
	36M	2,167	2,466	2,363	2,372	0,035	0,0660	2,79
	Comparison (significant differences)							
				chi ² =7,582; p=0,055				
				12 with 36: z=2,370; p<0,05				
				24 with 36: z=2,159; p<0,05				
BAG	0M	2,358	2,507	2,427	2,426	0,015	0,0355	1,46
	12M	2,329	2,503	2,432	2,448	0,041	0,0498	2,05
	24M	2,268	2,518	2,418	2,428	0,034	0,0585	2,42
	36M	2,198	2,506	2,351	2,348	0,070	0,0823	3,50
	Comparison (significant differences)							
				chi ² =14,645; p<0,01				
				0 with 36: z=3,616; p<0,001				
				12 with 36: z=4,325; p<0,001				
				24 with 36: z=3,163; p<0,01				
BBM	0M	2,316	2,480	2,410	2,422	0,031	0,0503	2,09
	12M	2,306	2,470	2,390	2,390	0,024	0,0408	1,71
	24M	2,195	2,442	2,354	2,387	0,064	0,0775	3,29
	36M	2,133	2,557	2,353	2,357	0,054	0,0996	4,23
	Comparison (significant differences)							
				chi ² =12,891; p<0,01				
				0 with 12: z=2,342; p<0,05				
				0 with 24: z=3,086; p<0,01				
				0 with 36: z=2,343; p<0,05				
				12 with 24: z=2,414; p<0,05				
ABG	0M	2,267	2,491	2,388	2,400	0,036	0,0641	2,68
	12M	2,296	2,476	2,396	2,413	0,052	0,0619	2,59
	24M	2,278	2,519	2,419	2,428	0,028	0,0529	2,19
	36M	2,275	2,441	2,363	2,360	0,028	0,0437	1,85
	Comparison (significant differences)							
				chi ² =7,070; p>0,05				
				12 z 36: z=2,314; p<0,05				
				24 z 36: z=3,024; p<0,01				
TCP	0M	2,262	2,467	2,382	2,384	0,030	0,0489	2,05
	12M	2,253	2,470	2,379	2,385	0,040	0,0537	2,26
	24M	2,204	2,463	2,360	2,389	0,047	0,0716	3,03
	36M	2,243	2,510	2,354	2,344	0,052	0,0732	3,11
	Comparison (significant differences)							
				chi ² =2,471; p>0,05 (no significant differences)				
REF	0M	2,300	2,486	2,386	2,402	0,037	0,0518	2,17
	12M	2,320	2,569	2,417	2,418	0,028	0,0596	2,47
	24M	2,210	2,464	2,377	2,397	0,072	0,0797	3,35
	36M	2,244	2,437	2,377	2,393	0,035	0,0590	2,48
	Comparison (significant differences)							
				chi ² =2,100; p>0,05 (no significant differences)				

AHA group after 36 months averages of FD values were significantly lower than in any previous periods of the study ($p < 0.001$; $p < 0.01$). In the group of BBM statistically significant differences were observed in consecutive periods of the study ($p < 0.01$). Comparison of results in pairs in different periods of the observation disclosed that there were, statistically significant differences between the values of FD at baseline and the values of FD in each of the subsequent periods ($p < 0.05$, $p < 0.01$). In this scope, a similarity to the NON group can be observed, however in the BBM group one more important difference appeared - significant decrease in FD values was observed in the examination after 24 months in comparison to values obtained after 12 months. In ABG group we found no statistically significant difference in FD values over analyzed period ($p > 0.05$). However, detailed comparison of pairs of FD values calculated for different periods disclosed that the averages obtained after 36 months were significantly lower than after 12 months ($p < 0.05$) and after 24 months ($p < 0.01$). There were no statistically significant differences in results over time ($p > 0.05$) in the TCP and REF groups. For better visualization above mentioned relations were presented in Figure 2.

A two factor analysis of variance (biomaterial and time) was performed and results presented in the Table 2. After 36 months, no statistically significant difference in FD values between the examined groups was observed ($p > 0.05$) (Figure 2). Statistically significant differences were noticed in all other periods of the study, both in the initial period, as well as after 12 months and 24 months ($p < 0.001$) (The Kruskal–Wallis one-way analysis of variance was performed). In the initial stage “00M” – state immediately after operation – FD averages calculated for the TCP was significantly lower than for the AHA group ($p < 0.05$) and for the BAG ($p < 0.01$). Results in other groups at baseline period did

not differ from each other in a statistically significant way ($p > 0.05$). After 12 months, it appeared that the TCP group differ significantly from the BAG group ($p < 0.01$) and from BBM and NON groups ($p < 0.05$). In the BAG group significantly higher FD values were observed on average than in other groups. Also during the examination after 24 months averages were significantly higher in this group than in the TCP and BBM ($p < 0.05$). In this study period (24 months) in the TCP group averages were significantly lower than in the ABG group ($p < 0.05$).

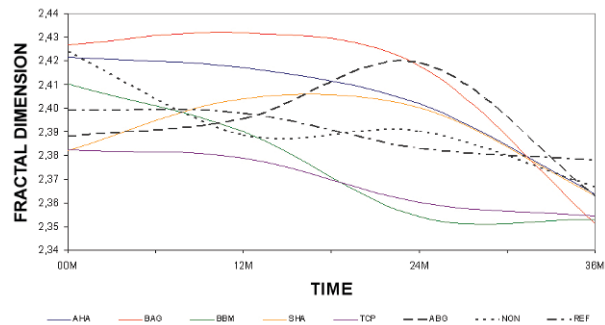


Figure 2. Fractal dimension in investigated groups. Abbreviations: 00M – state immediately after operation, 12M – twelve months after surgery, 24M – twenty four months after surgery, 36M – thirty six months after surgery. AHA - Slow alterations in ROI lead in final observation to less heterogenous texture of implantation site. BAG – Gradual, slow homogenization of internal structure of implantation site, finally done significantly simpler texture. BBM – the most noticeable changes were observed during first year after implantation, significantly more homogenous radiotexture was stable two and next three years post-operationally. SHA – Heterogenous texture begun to be visible in 12M and 24M, and statistically significance its decrease was confirmed at 36M. TCP – Texture alteration was not confirmed during 36 month post-operational observation in this study. ABG – Relatively not complex trabecular had only peak at final phase of remodeling period [24M].

Table 2. Comparison of results between the groups in the different time points

Examination time	Value of the Kruskal–Wallis one-way analysis of variance	Statistical significance p	Significant differences between groups	The value of z test	Statistical significance p
0M	26.476	$p < 0.001$	AHA with TCP BAG with TCP	3.205 3.602	$p < 0.05$ $p < 0.01$
12M	26.236	$p < 0.001$	BAG with TCP BAG with BBM BAG with NON	4.098 3.353 3.435	$p < 0.01$ $p < 0.05$ $p < 0.05$
24M	22.890	$p < 0.001$	BAG with TCP BAG with BBM TCP with ABG	3.450 3.338 3.126	$p < 0.05$ $p < 0.05$ $p < 0.05$
36M	2.970	$p > 0.05$	(no significant differences)		

Abbreviations: REF – reference bone, NON – spontaneously healed bone defect, ABG – autogenous bone graft, AHA – algae derived hydroxyapatite, BAG – biological active glass, BBM – bovine bone mineral, SHA – synthetic hydroxyapatite, TCP – beta – tricalcium phosphate, 00M – state immediately after operation, 12M – twelve months after surgery, 24M – twenty four months after surgery, 36M – thirty six months after

4. Discussion

In this paper, we analyzed the structural pattern of bone regeneration after the implantation of different bone substitute materials by means of the fractal. ShROUT et al. [1] state that results of a fractal analysis of alveolar bone may be affected by ROI size and shape, but in our study all ROI were standardized and had sizes of 64x64 pixels, and were only limited by the neighborhood of a tooth, implants and sinus. Moreover, in present research, all digital radiographs were standardized and projection of images did not influence the FD. Thus, this factor did not influence the results of our study. Optical density of the radiograph, geometric projection, and the direction in which the bone trabeculae are placed have no bearing on the value of the method of a fractal analysis. It can serve as a research tool in helping to evaluate the bone structure in all healing periods, as well as to assess the bone healing factor. The fractal dimension method is an effective tool for the description of the dynamics of bone remodeling by bone substitutes and bone resorption, and is useful as a quantitative indicator for these processes [50,51]. It is known that similar values of the fractal measurement in the location of the biomaterial implantation and referential bone indicate the presence of the correct bone structure. Therefore, fractal measurement reflects the number of bone trabeculae and their correct arrangement.

Veltri et al. discover in animal model that fractal dimension is potentially useful to evaluate bone quality at implant sites preoperatively and noninvasively [52]. Koyama et al. also show that FD is closely correlated with bone mineral density. These results suggest that a fractal analysis of bone images is a useful, non-invasive method for assessing bone strength, and the strength of a newly formed bone [53]. It is important especially in controlling large bone defects after application of bone filling material. Non-invasive assessment of FD could be used to monitor the results of a surgery and the use of bone substitutes over long periods of time.

The healing of bone tissue entails two parallel processes, i.e. resorption and osteogenesis. After fifteen weeks, in the place of a healing bone defect, a woven bone forms, which duly transforms into a mature bone. This process lasts approximately twelve months. Finally trabeculae arise as a result of pulling and pressure [54]. The system of trabeculae determines the degree of texture organization which can be evaluated on the basis of the fractal. NON group presented the detection of normal bone wall visualization between defect and registration plate. This is the feature of method of conduction of this study [intra-oral periapical radiography]. During healing and remodeling which involved

surrounding bone the structure observed in radiographs quickly became apparent. Processes that took place in the regions of biomaterial placement and in a spontaneously healing wound, in the span of 36 months, led in consequence to similar systematization to a dense bone - FD values did not differ significantly (despite of TCP). This means that the distribution of trabeculae was regular to a similar extent. These processes were time dependent. It seems that lack of the difference between FD values for TCP within the time of observation is connected with the resorption of the TCP particles and also with rapid osteogenesis (TCP gained similar FD values like REF). It is known that Alpha-tricalcium phosphate bone cement is a material composed by calcium and phosphate and presents biochemical characteristics similar to the bone mineral phase [55]. Granules of TCP are recognized by utilized method as similar particles as normal bone trabeculae [bigger than BAG and smaller than AHA particles], and next the combination of rapid resorption with simultaneous new bone formation [25] protect the detection of texture alteration during the follow-up. Final product of that bone regeneration has feature of compact bone. Similar findings was obtained in semi-quantitative radiographic research – the inside three dimensional porous structure of TCP simulates the natural bionic bone structure [56]. On the basis of fractal analysis there is no possibility to differentiate the implantation site with spontaneously bone regeneration (the vertices of TCP leave the same FD structure as trabeculae of regenerated bone).

In case of filling a bone defect with an autogenic graft, regeneration is the consequence of three mechanisms: osteogenesis, osteoinduction and osteoconduction. In the process of healing, the whole transplanted bone is subject to gradual resorption and is simultaneously revitalized. The process of complete healing of an autogenic bone transplant lasts from six to twelve months [57]. Synthetic products can be efficient alternatives to autogenic, allogeneic, or xenogenic grafts [26]. Similar processes arise when augmentation is based on the alloplastic material. Some authors, however indicate that alloplastic grafts i.e. hydroxylapatite bone grafts present more intense neo-osteogenic process in comparison to allogenic grafts [58].

High dynamics of regeneration of the bone tissue takes place within the first year after implanting the biomaterials. The newly formed bone differs in its structure, as its trabeculae are different from the surrounding bones. The results of our study indicate significant differences in the dynamics of resorption and osteoconducting between different groups of bone substitute materials.

AHA and BAG demonstrated gradual simplification of the own texture in implantation site down to reference

values [REF, NON, ABG] in 36M. On one hand it is the resorption effect, and on the other hand it is new bone conduction within a scaffold of biomaterial in jaw bone defect. Synthetic hydroxylapatite [SHA] is stable after intraosseal application. Only in 36-month examination decrease of structure complexity was noticed. Small porosity and crystal composition may determine such as long-time constancy. Generally a similar pattern of structural evolution of BBM to reference defect [NON] derived of origin of biomaterial. It is just deproteinized cancellous bone. Thus, the structure of biomaterial is like normal trabecular bone - well detected in NON group [as covering wall of the defect]. But interaction between the biomaterial with host bone is more complicated. Because of strong osteoconductivity, [8,59] the amount of new bone formed inside the BBM scaffold is great enough to merge particles of biomaterial in solid block of hard tissue. That block is relatively monolithic what is described by the lowest revealed in this study FD value which was 2.353. BBM is considered as non-resorbable material because several years (3–6 years) after implantation it is still unresorbed [10]. The presence of residual particles within the newly formed bone is inadvisable because it interferes with its growth and affects the properties of the resulting tissue, and influences its osteointegration capacity for dental implants [59,60].

The fast changes during six to eight months, described by many authors, (complete resorption when implanted in humans) [25,61] maybe though proved in our study. Tamimi indicates that the new bone at the site of biomaterial implantation differs from the intact one after 24 months and it still differs at the maximum recorded time of 36 months after the surgery [62]. This suggests that another long-term histological study is necessary to investigate the issue. No differences between structural pattern after BAG implantation were observed between time intervals 00M and 12M. In addition, 12 and 24M may suggest that BAG was resorbed within the first two years after surgery and within the next year the residual bone defect was remodeled and healed. It is important to realize that, thanks to the late resorption [AHA, SHA,

BAG], these bone substitutes remain stable and prevent tissue collapse, which is important for today's oral implantology i.e. soft tissue esthetics.

The results show that the fractal dimension can detect differences in newly formed bone structure filled with different bone replacement materials over time. Differences in fractal dimensions between implanted bone substitutes provide information on how and at what time the cancellous bone filled with various replacement materials remodels the defects.

This study shows that fractal analysis can characterize the morphological complexity of each bone substitute during the remodeling process by measuring the fractal dimensions. This enables a new understanding of how change in cancellous bone structure may occur as a result of bone filling materials. The fractal method described in this study can be used for assessing trabecular remodeling and resorption. The method proposed is non-invasive. It is not a burden to the patient and, at the same time it helps to obtain information regarding bone microstructure and the assessment of the kinetics taking place inside the bone tissue and in comparing their pictures with those of the intact bone. Fractal technique can describe bone substitutes.

5. Conclusions

On the basis of the differences in the dynamics of alteration among different bone substitute materials, we can distinguish two groups. Visible changes in the structure emerge earlier in places of implantation of BBM versus to the group of biomaterials constituting more stable patterns of radiotexture: AHA, BAG, SHA. As far as the fractal dimension is concerned, TCP is nonrecognisable contrary to reference bone because of high resorption rate. More complex structures of this series of bone substitutes finally transforms into more simplex site by influence of surrounded vital bone - fractal normal bone. Fractal analysis revealed that final bone regeneration in implantation sites can lead to total healing, but requires a long time [approximately 36 months].

References

- [1] Shrouf MK, Potter BJ, Hildebolt CF. The effect of image variation on fractal dimension calculations. *Oral Surg Oral Med Oral Pathol Oral Radiol Endod* 1997; 84: 96–100
- [2] Tatum H. Maxillary and sinus implant reconstructions. *Den Clin North Am* 1986; 30: 207–229
- [3] Pappalardo S, Puzzo S, Carlino V, Cappello V. Bone substitutes in oral surgery. *Minerva Stomatol* 2007; 56: 541–557
- [4] Boyne PJ, James RA. Grafting of the maxillary sinus with autogenous marrow and bone. *J Oral Surg* 1980; 38: 613–616
- [5] Wood RM, Moore DL. Grafting of the maxillary sinus with intraorally harvested autogenous bone prior to implant placement. *Int J Oral and Maxillofac Implants* 1988; 3: 209–214
- [6] Harris WH, White RE, McCarthy JC, Walker PS, Weinberg EH. Bony ingrowth fixation of acetabular component in canine hip joint arthroplasty. *Clin Orthop Relat Res* 1983; 176: 7–11
- [7] Hulbert SF, Young FA, Mathews RS, Klawitter JJ, Talbert CD, Stelling FH. Potential of ceramic materials as permanently implantable skeletal prostheses. *J Biomed Mater Res* 1970; 4: 433–456
- [8] Kozakiewicz M, Handlik M, Arkuszewski P, et al. Bone augmentation with Bio-OSS. 18 month assessment utilizing radiological subtraction. *Zeitschrift Zahnärztlich Implantologie* 2001, suppl, S14
- [9] Holinger J O, Brekke J, Gruskin E, Lee D. Role of bone substitutes. *Clin Orthop Relat Res* 1996; 324: 55–65
- [10] Taylor JC, Cuff SE, Leger JP, Morra A, Anderson GI. In vitro osteoclast resorption of bone substitute biomaterials used for implant site augmentation: a pilot study. *Int J Oral Maxillofac Implants* 2002; 17: 321–330
- [11] Wheeler DL, Stokes KE, Hoelrich RG, Chamberland DL, McLoughlin SW. Effect of bioactive glass particule size on osseous regeneration of cancellous defects. *J Biomed Mater Res* 1998; 41: 527–533
- [12] Lovelace TB, Mellonig JT, Meffert RM, Jones AA, Nummikoski PV, Cochran DL. Clinical evaluation of bioactive glass in the treatment of periodontal osseous defects in humans. *J Periodontol* 1998; 69: 1027–1035
- [13] Zins JE, Whitaker LA. Membranous versus endochondral bone: implications for craniofacial reconstruction. *Plast Reconstr Surg* 1983; 72: 778–785
- [14] Sailer HF, Weber FE. Bone substitutes. *Mund Kiefer Gesichtschir* 2000; 4: 384–391
- [15] Moy PK, Lundgren S, Holmes RE. Maxillary sinus augmentation: histomorphometric analysis of graft materials for maxillary sinus floor augmentation. *J Oral Maxillofac Surg* 1993; 51: 857–862
- [16] Tadjoeidin ES, de Lange GL, Holzmann PJ, Kulper L, Burger EH. Histological observations on biopsies harvested following sinus floor elevation using a bioactive glass material of narrow size range. *Clin Oral Implants Res* 2000; 11: 334–344
- [17] Aygit AC, Sarikaya A, Candan L, Ayhan MS, Cermik TF. Comparison of alloplastic implants for facial bones by scintigraphy and histology: an experimental study. *Eur J Plast Surg* 1999; 22: 102–106
- [18] Hanisch O, Lozada JL, Holmes RE, Calhoun CJ, Kan JY, Spiekermann H. Maxillary sinus augmentation prior to placement of endosseous implants: a histomorphometric analysis. *Int J Oral Maxillofac Implants* 1999; 14: 329–336.
- [19] Yildirim M, Spiekermann H, Biesterfeld S, Edelhoff D. Maxillary sinus augmentation using xenogenic bone substitute material Bio-Oss in combination with venous blood. A histologic and histomorphometric study in humans. *Clin Oral Implants Res* 2000; 11: 217–229
- [20] Jensen T, Schou S, Svendsen PA, Forman JL, Gundersen HJ, Terheyden H, Holmstrup P: Volumetric changes of the graft after maxillary sinus floor augmentation with Bio-Oss and autogenous bone in different ratios: a radiographic study in minipigs. *Clin Oral Implants Res*. 2012; 23(8): 902-910
- [21] Jensen T, Schou S, Stavropoulos A, Terheyden H, Holmstrup P. Maxillary sinus floor augmentation with Bio-Oss or Bio-Oss mixed with autogenous bone as graft in animals: a systematic review. *Int J Oral Maxillofac Surg* 2012; 41: 114-120
- [22] McAllister BS, Margolin MD, Cogan AG, Buck D, Hollinger JO, Lynch SE. Eighteen-month radiographic and histologic evaluation of sinus grafting with anorganic bovine bone in the chimpanzee. *Int J Oral Maxillofac Implants* 1999; 14: 361–368.
- [23] Liu YL, Schoenaers J, De Groot K, de Wijn JR, Schepers E. Bone healing in porous implants: a histological and histometrical comparative study on sheep. *J Mater Sci Mater Med* 2000; 11: 711–717
- [24] Haas R, Baron M, Donath K, Zechner W, Watzek G. Porous hydroxyapatite for grafting the maxillary sinus: a comparative histomorphometric study in sheep. *Int J Oral Maxillofac Implants* 2002; 17: 337–346
- [25] Suba Z, Takács D, Gyulai-Gaál Sz, Kovács K.

- Facilitation of beta-tricalcium phosphate-induced alveolar bone regeneration by platelet-rich plasma in beagle dogs. A histologic and histomorphometric study. *Int J Oral Maxillofac Implants* 2004; 19: 832–838
- [26] Almasri M, Altalibi M. Efficacy of reconstruction of alveolar bone using an alloplastic hydroxyapatite tricalcium phosphate graft under biodegradable chambers. *Br J Oral Maxillofac Surg* 2011; 49: 469–473
- [27] Anselme K, Noel B, Flautre B, Blary MC, Delecourt C, Descamps M. Association of porous hydroxyapatite and bone marrow cells for bone regeneration. *Bone* 1999; 25: 51–54
- [28] Laurencin CT, Attawia MA, Elgendy HE, Herbert KM. Tissue engineered bone regeneration using degradable polymers: the formation of mineralized matrices. *Bone* 1996; 19: 93–99
- [29] Bassil J, Naaman N, Lattouf R, Kassis C, Changotade S, Baroukh B, Senni K, Godeau G: Clinical, histological, and histomorphometrical analysis of maxillary sinus augmentation using inorganic bovine in humans: preliminary results. *J Oral Implantol*. 2013; 39(1): 73–80
- [30] Isenberg G, Goldman HM, Spira J, Parsons FG, Street PN. Radiography analysis by two-dimensional microdensitometry. *J Am Dent Assoc* 1968; 77: 1069–1073
- [31] Ort MG, Gregg EC, Kaufman B. Subtraction radiography: techniques and limitations. *Radiology* 1977; 124: 65–72
- [32] Ruttimann UE, Ship JA. The use of fractal geometry to quantitate bone structure from radiographs. *J Dent Res* 1990; 69: 287 (Abstr 1431)
- [33] Yasar F, Akgunlu F. The differences in panoramic mandibular indices and fractal dimension between patients with and without spinal osteoporosis. *Dentomaxillofac Radiol* 2006; 35: 1–9
- [34] Chen J, Zheng B, Chang YH, Shaw CC, Towers JD, Gur D. Fractal analysis of trabecular patterns in projection radiographs. An assessment. *Invest Radiol* 1994; 29: 624–629
- [35] Ruttimann UE, Webber RL, Hazelrig JB. Fractal dimension from radiographs of peridental alveolar bone. *Oral Surg Oral Med Oral Pathol* 1992; 74: 98–110
- [36] Law AN, Bollen AM, Chen SK. Detecting osteoporosis using dental radiographs: a comparison of four methods. *J Am Dent Assoc* 1996; 127: 1734–1742
- [37] Samarabandu J, Acharya R, Hausmann E, Allen K. Analysis of bone X-rays using morphological fractals. *IEEE Trans Med Imaging* 1993; 12: 466–470
- [38] Geraets WGM, van der Stelt PF. Fractal properties of bone. *Dentomaxillofac Radiol* 2000; 29: 144–153
- [39] Webber RL, Hazelrig JB, Patel JR, Van den Berg HR, Lemons JE. Evaluation of site-specific differences in trabecular bone using fractal geometry. *J Dent Res* 1991; 70: 528 (Abstr 2095)
- [40] Shroud MK, Potter BJ, Hildebolt CF. The effect of image variations on fractal dimension calculations. *Oral Surg Oral Med Oral Pathol Oral Radiol Endod* 1997; 84: 96–100
- [41] Jolley L, Majumdar S, Kapila S. Technical factors in fractal analysis of periapical radiographs. *Dentomaxillofac Radiol* 2006; 35: 393–397
- [42] Shroud MK, Roberson B, Potter BJ, Mailhot JM, Hildebolt CF. A comparison of 2 patient populations using fractal analysis. *J Periodontol* 1998; 69: 9–13
- [43] Wilding RJ, Slabbert JC, Kathree H, Owen CP, Crombie K, Delport P. The use of fractal analysis to reveal remodelling in human alveolar bone following the placement of dental implants. *Arch Oral Biol* 1995; 40: 61–72
- [44] Veenland JF, Grashius JL, van der Meer F, Beckers AL, Gelsema ES. Estimation of fractal dimension in radiographs. *Med Phys* 1996; 23:585–594
- [45] Caligiuri P, Giger ML, Favus M. Multifractal radiographic analysis of osteoporosis. *Med Phys* 1994; 21: 503–508
- [46] Cargill EB, Barrett HH, Fiete RD, Ker M, Patton D, Sweeley GW. Fractal physiology and nuclear medicine scans. *SPIE Conference on Medical Imaging II* 1988; 355–362
- [47] Kozakiewicz M, Bogusiak K, Hanclik M, Denkowski M, Arkuszewski P. Noise In subtraction images made from pairs of intraoral radiographs: a comparison between four methods of geometric alignment. *Dentomaxillofac Radiol* 2008; 37:40–46
- [48] Chan KL. Quantitative characterization of electron micrograph image using fractal feature. *IEEE Trans Biomed Eng* 1995; 42: 1033–1037
- [49] Wojtowicz A, Chaberek S, Urbanowska E, Ostrowski K. Comparison of efficiency of platelet rich plasma, hematopoieic stem cells and bone marrow in augmentation of mandibular bone defects. *N Y State Dent J* 2007; 73: 41–45
- [50] Berry JL, Towers JD, Webber RL, Pope TL, Davidai G, Zimmerman M. Change in trabecular architectures measured by fractal dimension. *J Biomech* 1996; 29: 819–822
- [51] Le Corroller T, Halgrin J, Pithioux M, Guenoun D, Chabrand P, Champsaur P. Combination of texture analysis and bone mineral density improves the prediction of fracture load in human femurs. *Osteoporos Int* 2012; 23: 163–169

- [52] Veltri M, Ferrari M, Balleri P. Correlation of radiographic fractal analysis with implant insertion torque in a rabbit trabecular bone model. *Int J Oral Maxillofac Implants* 2011; 26: 108-114
- [53] Koyama A, Kumasaka S, Kashima I. Relationship between bone mineral density and 2D and 3D structural parameters of bone trabeculae. *Oral Radiology* 2005; 21: 62-68
- [54] Meagher PJ, Morrison WA. Free fibula flap-donor-site morbidity: case report and review of the literature. *J Reconstr Microsurg* 2002; 18: 465-468
- [55] Tsuji RK, Jorgetti V, Bento RF, Brito Neto RV. Use of Alpha-tricalcium Phosphate Bone Cement in the Surgical Treatment of Mastoid Cavity. *Int Arch Otorhinolaryngol* 2008; 12: 397-405
- [56] Sang H, Wang Z, Guo Z, Wang L, Li J, Meng G, et al. Clinical results and the mechanism of bone healing for the repair of bone defects due to tumor resection with novel interporous TCP. *Zhongguo Xiu Fu Chong Jian Wai Ke Za Zhi* 2008; 22: 463-467 (Abstract)
- [57] Marx RE. Bone and bone graft healing. *Oral Maxillofac Surg Clin North Am* 2007; 19: 455-466
- [58] Mamun S, Akhter M, Molla MR. Bone Grafts in Jaw Cysts- Hydroxyapatite & Allogenic Bone – A Comparative Study. *BSMMU J* 2009; 2: 34-39
- [59] Zaffe D, Leghissa GC, Pradelli J, Botticelli AR. Histological study on sinus lift grafting by Fisiograft and Bio-Oss. *J Mater Sci Mater Med* 2005; 16: 789-793
- [60] De Boever AL, De Boever JA. Guided bone regeneration around non-submerged implants in narrow alveolar ridges: a prospective long-term clinical study. *Clin Oral Implants Res* 2005; 16: 549-556
- [61] Wiltfang J, Schlegel KA, Schultze-Mosgau S, Nkenke E. Sinus floor augmentation with beta-tricalcium phosphate (beta-TCP): does platelet-rich plasma promote its osseous integration and degradation? *Clin Oral Implants Res* 2003; 14: 213-218
- [62] Tamimi FM, Torres J, Tresguerres I, Clemente C, López-Cabarcos E, Blanco LJ. Bone augmentation in rabbit calvariae: comparative study between Bio-Oss and a novel β -TCP/DCPD granulate. *J Clin Periodontol* 2006; 33: 922-928